

Electron Showers of High Primary Energy in Lead*

Dietrich Müller

Enrico Fermi Institute and Department of Physics, University of Chicago, Chicago, Illinois 60637

(Received 28 February 1972)

The development of electron cascade showers in a lead-scintillator sandwich of 8 plastic scintillators in about 20 radiation lengths of lead has been investigated. This detector, which was used for cosmic-ray studies, has been calibrated with electrons with energies from 2 to 15 GeV at SLAC. Measured shower profiles are presented, and expressions are given which allow an extrapolation of the measured data up to energies around 1000 GeV. The results are compared with analytical shower theories and Monte Carlo calculations.

I. INTRODUCTION

The development of electron-photon cascades has been studied for several decades because of its importance for cosmic-ray and high-energy physics. In general, considerable discrepancies between experimental data and analytically calculated values have been found, while Monte Carlo calculations seem to agree much better with the measurements. Most of the published experiments¹⁻⁶ have, however, been restricted to primary energies around 1 GeV or less. Hence, a detailed description of shower phenomena at higher energies which is supported by measurements is still needed.

The purpose of this paper is to report new measurements of electron-induced showers in lead with primary energies up to 15 GeV and methods of extrapolation of the observed shower profiles to extremely high energies. This research has been stimulated by an experiment which is aimed at measuring the flux and energy spectrum of cosmic-ray electrons up to energies around 1000 GeV. In high-altitude balloon flights we have exposed a cosmic-ray telescope whose main element is a lead-scintillator sandwich, and we have carried out calibration measurements with this detector at the Stanford Linear Accelerator.

In the following we shall describe and discuss the shower data as obtained with this instrument at SLAC. The procedures used in evaluating actual cosmic-ray data will be reported elsewhere.⁷

II. EXPERIMENTS

Figure 1 shows a schematic cross section of the shower detector. Incoming particles traverse first a counter telescope (plastic scintillator and gas Čerenkov counters, not shown in Fig. 1) and then enter a lead-scintillator sandwich consisting of 8 plastic scintillators $D1, \dots, D8$ (NE110, 0.25 in. thick each) and lead plates (purity 99.9%). The

thickness of the first lead plate is 1 radiation length (r.l.), all following plates are 2.5 r.l. thick. Underneath the bottom counter $D8$ a lead plate of 2-r.l. thickness is located in order to surround also counter $D8$ with lead. Throughout this paper we accept the following value⁸ for lead: 1 r.l. = 0.57 cm or 6.4 g/cm². Each scintillator with its housing is about 0.025 r.l. thick, and the total amount of material in front of the sandwich (including beam defining counters, etc.) is about 0.2 r.l. The sandwich has conical shape, its diameter increasing from 49 to 72 cm.

Each scintillator is viewed through Lucite light pipes by several photomultiplier tubes (2 tubes each are used for scintillators $D1, \dots, D4$, and 3 tubes each for $D5, \dots, D8$). The signals from the photomultiplier tubes after being summed for each scintillator are processed by eight pulse-height analyzers. In this manner, the pulse-height profile for each event is measured at 8 depths, increasing from 1.2 r.l. ($D1$) to 18.9 r.l. ($D8$) (including the material in front of the sandwich and of the counters themselves), with spacings of 2.5 r.l. of lead. The over-all resolution of an individual scintillation counter for relativistic muons is

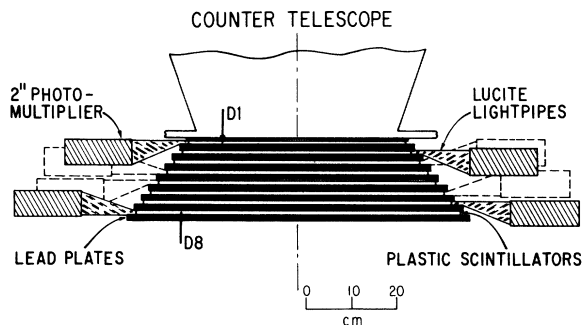


FIG. 1. Schematic cross section of the lead-scintillator sandwich. The detector is rotationally symmetric with respect to the central axis.

about 40–50% [full width at half maximum (FWHM)].

In a series of calibration measurements the detector system has been exposed to electrons from 2 to 15 GeV/c momentum at the Stanford Linear Accelerator. We had available a secondary beam from a Be target ("C-beam") which contained a small pion contamination (<10%). In most runs this electron beam was collimated to an area of 5×10 cm, and had a momentum spread over this area of less than $\pm 3\%$.

Measurements were carried out with the beam either parallel and close to the detector axis, or under an angle of 25° with respect to the detector axis. If not otherwise stated the results which are reported in the following refer to electrons traversing the detector parallel to its axis.

For calibration purposes, some measurements with pions were made as well. The signal corresponding to the *average* energy loss of penetrating pions of 10 GeV was determined for each individual scintillator. From these values, the average signal of electrons of 7.4 MeV (critical energy in lead) was calculated and was then used to normalize all further pulse-height readings.

III. RESULTS

Figure 2 shows some of the results of a typical run at a primary energy $E_0 = 14$ GeV. After sort-

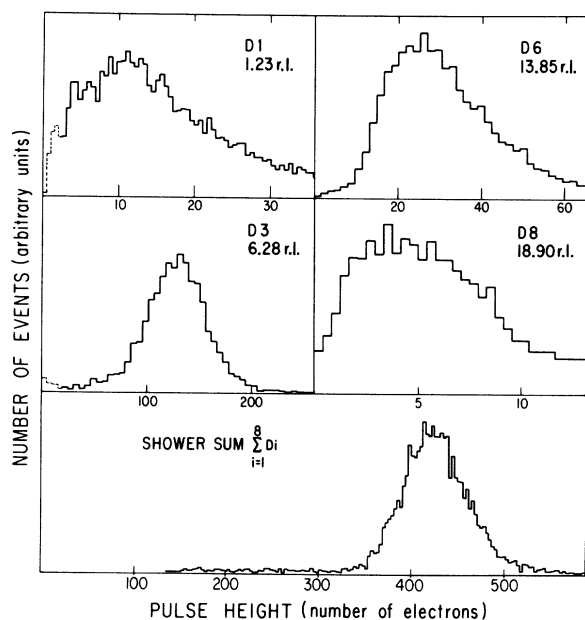


FIG. 2. Pulse-height distributions at 4 different depths of the sandwich and distribution of the sum of all 8 counters (shower sum) for primary electrons with $E_0 = 14$ GeV.

ing out the pion background, the measured pulse-height distributions produced by about 7000 primary electrons in 4 of the scintillation counters are plotted. (The pulse heights are given in units of the average energy loss of single electrons of 7.4 MeV.) Also plotted as a measure of the total path length of each shower is the distribution of the sum of all 8 pulse heights for each event (in the following called shower sum). Qualitatively, it can be seen from this figure that the distributions become symmetric for large average pulse heights (≥ 40 electrons), and that the distribution of the shower sum is much sharper (17% FWHM) than the distributions from individual counters (40 to $>100\%$ FWHM).

Therefore, as expected, the shower sum turns out to be a very good measure for the energy of incoming electrons. In Fig. 3 we have plotted the average shower sum vs the energy, which exhibits a practically linear relationship in this energy region. Obviously, the energy of the incoming electrons is largely dissipated within the detector.

The energy resolution of the detector as obtained from the distributions of the shower sum is plotted in Fig. 4. It seems to improve slightly with increasing energy. The pulse-height distributions as measured with individual counters depend essentially only on the average signal in these counters, independent of the primary energy and regardless of whether the signal is measured in the rising part or in the tail of the shower profile. The width of these distributions is larger than one would expect for pure Poisson distributions, which can be partially explained by Landau broadening. This is illustrated in Fig. 5, where we have plotted the

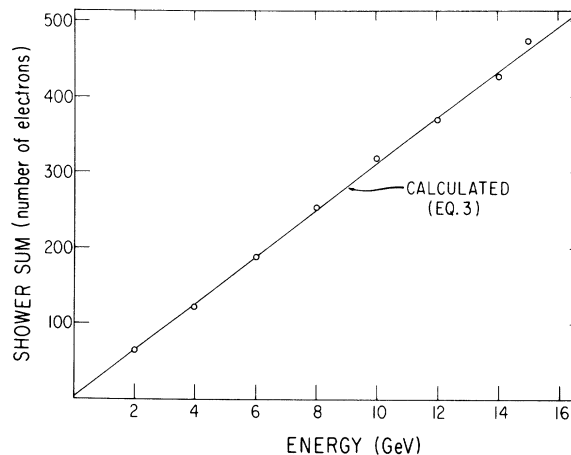


FIG. 3. Average shower sum measured as a function of the primary energy E_0 . The solid line is calculated as described in Sec. IV.

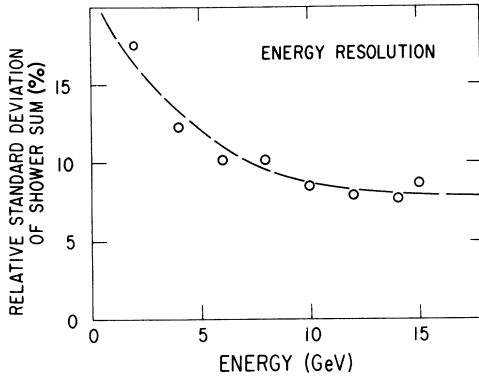


FIG. 4. Energy resolution of the detector in terms of the relative standard deviation of the shower sum vs the primary energy E_0 .

resolution of individual scintillators as a function of the average shower signal.

Figure 6 shows the average shower profiles for different energies as obtained in these calibration measurements for electron beams parallel to the axis of the detector. If the beam traverses the detector under an angle ϕ with respect to the axis, one expects the corresponding shower profile to be compressed by a factor $1/\cos\phi$ (since more matter is traversed) and enhanced by the same factor (since the path length of the shower electrons in the scintillators is larger). This expectation is in very good agreement with the observations.

IV. ANALYTIC EXPRESSIONS FOR THE SHOWER PROFILES AND EXTRAPOLATION TO HIGHER ENERGIES

Most importantly, this study is aimed at obtaining analytic expressions for the observed shower profiles which can be unambiguously extrapolated and yield the shape of showers corresponding to much higher primary energies, up to around 1000 GeV. In other words, for energies which are presently not accessible with accelerators, a physically meaningful function $P(E_0, t)$ has to be determined, which depends explicitly only on the primary energy E_0 and on the depth of the material, t . This function must, of course, fit the measured profiles to a high degree of accuracy, and thereby justify its use to predict the profiles of high energy showers. None of the shower functions which have been obtained from analytical shower theories⁸⁻¹⁰ provides a sufficiently good fit to our data. However, we have been able to modify the expressions given as approximation A of Rossi and Greisen¹⁰ in such a way that they meet our requirements extremely well.

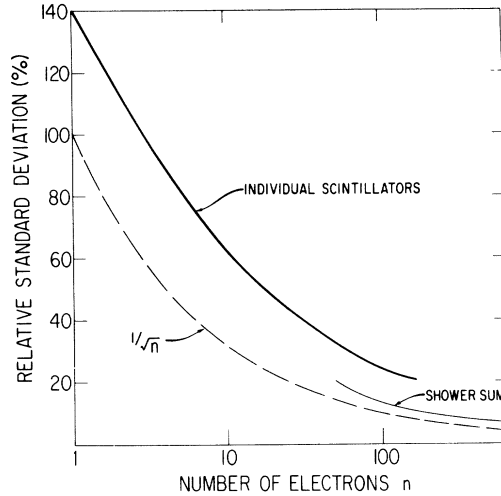


FIG. 5. Resolution of the individual scintillators for shower signals in terms of the relative standard deviation vs the signal height n . For comparison, the resolution of the shower sum is shown as well as $\sigma/n = 1/\sqrt{n}$, the relative standard deviation of a Poisson distribution.

In approximation A the following parametric equation is obtained for the number of shower electrons $\Pi_A(E_0, E^*, t)$ of energies larger than the cut-off energy E^* (kinetic energy) at a depth t (in r.l.), for a primary energy E_0 :

$$\Pi_A(E_0, E^*, t) = \left\{ \frac{H(s)}{(2\pi)^{1/2} [\lambda''(s)t + 1/s^2]^{1/2}} \right\} \times \frac{1}{s} \left(\frac{E_0}{E^*} \right)^s \exp[\lambda(s)t]. \quad (1a)$$

Hereby, the "age parameter" s is a quantity which increases with increasing absorber thickness and which is unity at the shower maximum. It is related to E_0 , E^* , and t as follows:

$$t = \frac{1}{\lambda'(s)} \left[\ln \left(\frac{E_0}{E^*} \right) - \frac{1}{s} \right] = f(E_0, E^*, s). \quad (1b)$$

The functions $H(s)$ and $\lambda(s)$ and its derivatives $\lambda'(s)$, $\lambda''(s)$ have been calculated and tabulated by Rossi and Greisen¹⁰ and by Nishimura.⁸

We have calculated the shower profiles according to these expressions by arbitrarily choosing $E^* = 7.4$ MeV (critical energy of electrons in lead⁸). We then determined the ratios of the measured and calculated profiles, P_m and Π_A , respectively:

$$\rho(E_0, t) = \frac{P_m(E_0, t)}{\Pi_A(E_0, E^*, t)}, \quad E^* = 7.4 \text{ MeV}. \quad (2)$$

It turns out that this ratio ρ becomes independent of the primary energy E_0 within the experimental

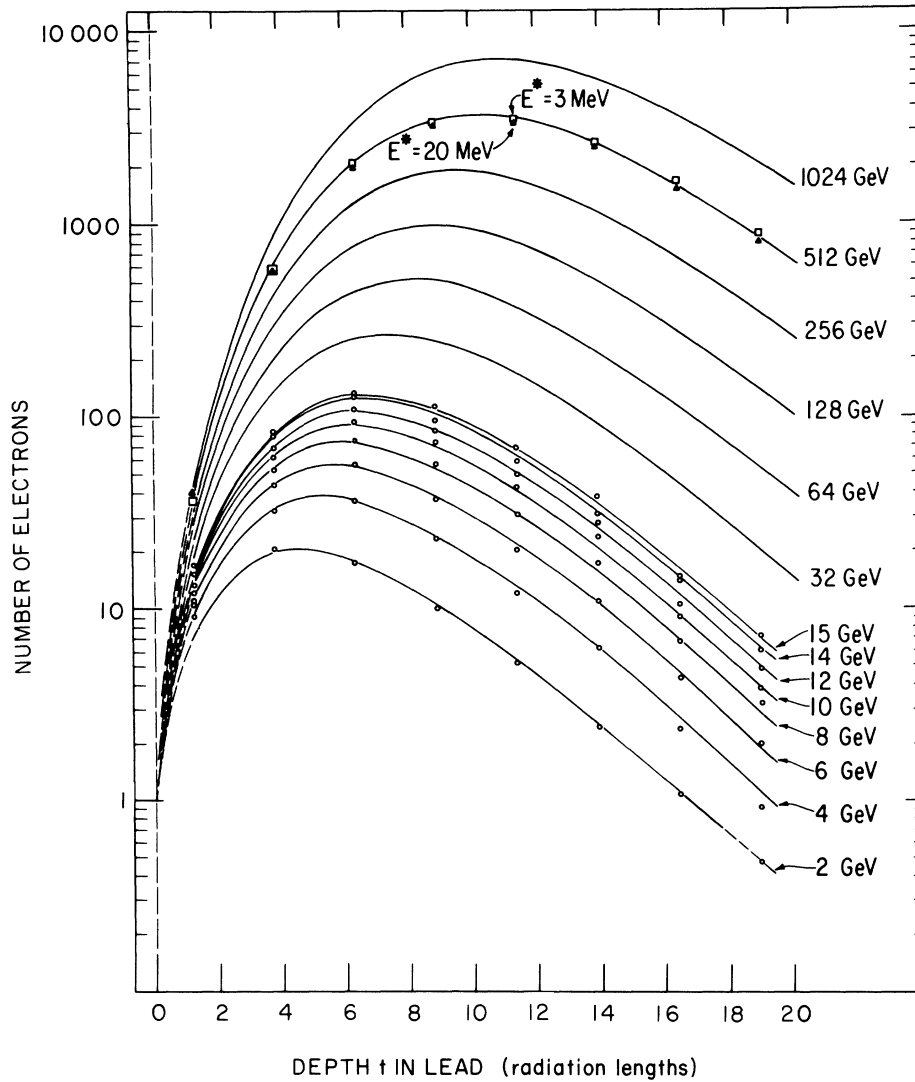


FIG. 6. Shower profiles in the energy region 2 to 1024 GeV. The data points at lower energies (2–15 GeV) are measured values, while the solid lines are calculated profiles according to the fitting procedure described in Sec. IV with $E^* = 7.4$ MeV. For 512 GeV, also calculated profiles with $\rho(s)$ corresponding to $E^* = 3$ MeV and 20 MeV are shown.

accuracy if we plot it as a function of the “age parameter” s . This function $\rho(s)$ is shown in Fig. 7.

Therefore, we propose the following expression for our shower profiles:

$$P(E_0, t) = \rho(s) \Pi_A(E_0, E^*, t), \quad (3)$$

$$E^* = 7.4 \text{ MeV}, \quad t = f(E_0, E^*, s).$$

We may interpret $\rho(s)$ as an empirical correction function to Eq. (1a) and (1b) which can be numerically determined from Fig. 7.

This expression represents an excellent fit to the measured shower profiles, as demonstrated in Fig. 6. The mean square deviation of the mea-

sured shower profile from the interpolated shower profile is $\sim 7\%$ for all energies and does not exhibit any noticeable energy dependence.

For the position t_{\max} and the height P_{\max} of the maxima of the shower profiles the following interpolation formulas are obtained from Eq. (3):

$$t_{\max} = 3.9 + \ln E_0, \quad (4)$$

$$P_{\max} = 10.71 E_0^{0.935}$$

$$(t \text{ in r.l., } E_0 \text{ in GeV}),$$

and the integral

$$S(E_0) = \int_0^{\infty} P(E_0, t) dt$$

is related to the energy E_0 by

$$S(E_0) = 76.2E_0. \quad (5)$$

Both relations (4) and (5) agree with the measured values within the experimental errors (compare Figs. 3 and 6).

It should be noted that the choice $E^* = 7.4$ MeV does not seem to be unique. Actually, the real cutoff energy of our detector is much smaller (see Sec. V). On the other hand, approximation A is not expected to yield good results for lead if $E^* < 20$ MeV.⁸ We may therefore choose a different value for E^* and try the same procedure as described for $E^* = 7.4$ MeV to fit our data. There-

by, we would obtain a new correction function $\rho(s)$ which depends again solely on the age parameter s but not on the energy E_0 . To demonstrate this result, we have plotted in Fig. 7 $\rho(s)$ for $E^* = 3$ MeV, 7.4 MeV, and 20 MeV. In Fig. 6 three corresponding extrapolated shower profiles for $E_0 = 512$ GeV are shown. Obviously, these profiles are almost identical. Hence, we feel justified to use expression (3) to extrapolate the shape of high-energy showers with good accuracy. Extrapolated shower profiles up to $E_0 = 1024$ GeV are shown in Fig. 6. While it seems to be difficult to estimate the possible error of these extrapolations, we believe that it is not larger than $\pm 15\%$.

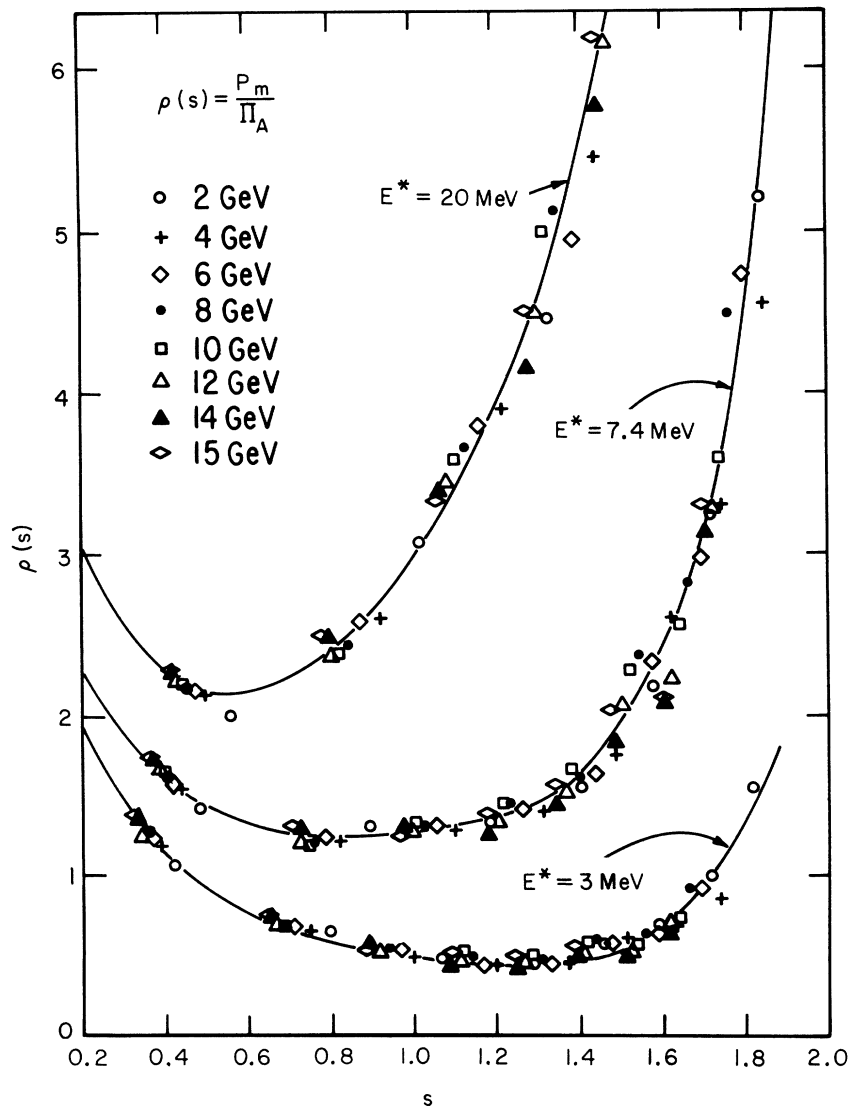


FIG. 7. Correction function $\rho(s) = P_m(E_0, t) / \Pi_A(E_0, E^*, t)$ for $E^* = 3, 7.4,$ and 20 MeV. The solid lines are fitted to the measured data points.

V. DISCUSSION

A detailed description of electron-photon cascades would involve knowledge of the energy spectra and of the angular and spatial distributions of all shower particles at any depth of the absorber. Obviously, our measurements do not contain sufficient information to reveal the complete shower phenomenon. Still, it is worthwhile to compare our data with results of Monte Carlo calculations¹¹⁻¹³ and of analytical shower theories.

Obviously, our data are related to the shower function $\Pi(E_0, E^*, t)$, the number of shower electrons with energies larger than the cutoff energy E^* produced by a primary electron of energy E_0 at a depth t of the absorber. However, our shower profiles do not directly represent the number of electrons in the shower, but rather are a measure of the collisional energy loss in the plastic scintillators in units of the energy loss of 7.4 MeV electrons. Also, our cutoff energy E^* does not seem to be very well defined.

We may assume that the average energy of a shower electron is equal to the critical energy of the absorber (7.4 MeV for lead, corresponding ionization loss in $\frac{1}{4}$ -in. scintillator of 1.23 MeV). This seems to be a reasonable approximation at least around the shower maximum, and, furthermore, the energy loss of electrons with differing energies will not be much different as long as they are able to penetrate the scintillators ($E \approx 1.3$ MeV). Electrons with $E < 1.3$ MeV, however, contribute only partially to our shower profiles. For example, a given number of 0.4 MeV electrons, would be counted only as about $\frac{1}{3}$ of this number. In order to determine an effective cutoff energy E^* for our detector, the energy spectrum of the shower electrons has to be known. Using the calculated spectra of Nagel¹¹ and Völkel¹² we determine for our experiment $E^* = 0.5 \pm 0.1$ MeV: Our shower profiles behave as if all electrons with kinetic energies ≥ 0.5 MeV contributed with equal weight.

In order to compare our data with recent Monte Carlo calculations we have plotted in Fig. 8 together with our results the function $\Pi(E_0, E^*, t)$ as calculated by Völkel¹² for $E_0 = 6$ GeV, the highest energy for which Monte Carlo data have been published. Obviously, the measured profile is significantly larger than the calculated shower. This discrepancy is partially explained by the fact that the cutoff energy used in the calculations is 1 MeV and therefore larger than our value of 0.5 MeV. However, at most a 10–15% increase may be expected due to the lower cutoff energy. To explain the remaining disagreement, we can no longer disregard the directions of the shower elec-

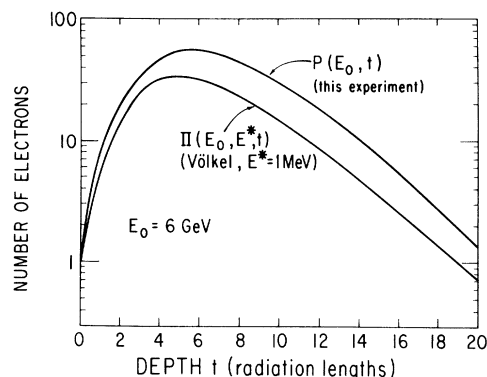


FIG. 8. Comparison of the shower profile $P(E_0, t)$ as obtained in this experiment with Monte Carlo data by Völkel (12) for $E_0 = 6$ GeV. The fact that Völkel uses a different value for the radiation length in lead has been taken into account.

trons: the signal produced by an electron traversing the scintillator under an angle θ with respect to the normal is proportional to $1/\cos\theta$.

Therefore our shower profiles do not describe the quantity $\Pi(E_0, E^*, t)$, but rather

$$P(E_0, E^*, t) = \Pi(E_0, E^*, t) \langle 1/\cos\theta \rangle,$$

where $\langle 1/\cos\theta \rangle$ is the average over all directions of the electrons at a given depth t .

Of course, we should not equate $\langle 1/\cos\theta \rangle$ with the correction function $\rho(s)$ as defined in Sec. IV. The expression of approximation A used there is known not to be a correct measure for the number of shower-electrons, particularly in the shower tail, where $\rho(s)$ therefore becomes rather large.

Assuming the Monte Carlo data describe $\Pi(E_0, E^*, t)$ accurately we obtain $\langle 1/\cos\theta \rangle \approx 1.8$ beyond the shower maximum. This number seems not to be inconsistent with the angular distributions from Monte Carlo calculations. It is somewhat larger than a value of 1.5 which would be expected for a $\cos^2\theta$ distribution of the shower electrons, and which has been indicated by measurements at lower energies.¹⁴

We can expect the integral

$$S(E_0) = \int_0^\infty P(E_0, E^*, t) dt$$

(see Sec. IV) to be an excellent measure of the total path length of the shower electrons. Due to the lateral spread of the shower electrons, the total path length must be larger than

$$\int_0^\infty \Pi(E_0, E^*, t) dt.$$

The $\cos\theta$ dependence of our data has however the effect that the lateral spread is correctly repre-

sented in $S(E_0)$.

We obtain $S(E_0) = CE_0$ with $C = 76.2$ r.l./GeV $\pm 5\%$. This number is only slightly smaller than the value of $C = 82.3$ r.l./GeV obtained from Monte Carlo calculations (for $E^* = 1$ MeV).¹¹ Approximation B of the analytical theory leads to $C = 135$ r.l./GeV for $E^* = 0$, and $C \approx 88$ r.l./GeV, if $E^* = 0.5$ MeV.⁸

The above interpretation of our data is only valid if we may disregard the transition effects which occur when the cascade propagates from lead into the scintillator material of much larger critical energy. Calculations¹⁵ predict that in this case the measured shower profiles may appear considerably depressed as compared to the true profiles in uniform material. However, since our scintillators are only 0.025 r.l. thick, we feel justified not to assume any serious distortion of our data due to this effect in agreement with recent measurements.¹⁶

Finally, we shall briefly comment on the function $\rho(s)$ which we have introduced in Sec. IV. A similar function $K(s, -s)$ has been used in approximation B of the shower theory in the method of Snyder and Serber (cited in Ref. 10). There the shower profile for $E^* = 0$ is given by

$$\Pi_B(E_0, 0, t) = \Pi_A(E_0, E_c, t)K(s, -s)$$

$$(E_c = 7.4 \text{ MeV}).$$

A graphic representation of $K(s, -s)$ is given by Rossi.¹⁰ The values of the functions $\rho(s)$ and $K(s, -s)$ appear to be significantly different. The discrepancies can be partially explained due to the angular spread of the shower electrons, the influence of multiple scattering, the energy dependence of the specific ionization of shower electrons, and due to the fact that the cutoff energy of our detector is not zero. Nevertheless, even if we try

to take all these effects into account, approximation B of the shower theory in this formulation does not provide a sufficient description of our data.

Summarizing our results we obtain the following conclusions:

(1) For all energies up to 15 GeV of the primary electron, both approximations (approximations A and B) of the classical shower theory fail to describe the measured shower development with sufficient accuracy.

(2) Within the experimental accuracy our measurements are essentially in agreement with predictions from recent Monte Carlo calculations concerning shower profiles, total path length, and average angular spread.

(3) Although a lead-scintillator sandwich does not directly give information on the number of electrons in the cascade, we can relate our shower profiles to the predicted profiles of approximation A of the shower theory by means of an empirical correction function $\rho(s)$, and, thereby, extrapolate the response of this shower detector up to very high energies. It is beyond the scope of this paper to discuss the physical meaning of $\rho(s)$ in detail.

ACKNOWLEDGMENTS

We appreciate the help of W. Johnson, E. Juliusson, G. Kelderhouse, and V. Kurtz, and of Mrs. H. Shaw and Mrs. N. Beck during the course of this experiment and the data analysis. We are indebted to Professor P. Meyer, Dr. R. Hartman, Dr. J. Faselow, and Dr. P. Schmidt for many valuable discussions, and we are grateful to the staff of SLAC, in particular to Dr. J. Murray and Dr. R. Gearhart for accommodating and helping us generously during the accelerator runs.

*Supported in part by the National Aeronautics and Space Administration under Grant No. NGL 14-001-005.

¹A. Kantz and R. Hofstadter, Phys. Rev. **89**, 607 (1953).

²C. A. Heusch and C. Y. Prescott, Phys. Rev. **135**, B772 (1964).

³E. Becklin and J. Earl, Phys. Rev. **136**, B237 (1964).

⁴G. Backenstoss, B. D. Hyams, G. Knop, and U. Stierlin, Nucl. Instr. and Methods **21**, 155 (1963).

⁵W. R. Nelson, T. M. Jenkins, R. C. McCall, and J. Cobb, Phys. Rev. **149**, 201 (1966).

⁶C. J. Crannell, Phys. Rev. **161**, 310 (1967).

⁷For preliminary results see P. Meyer and D. Müller, paper presented at the Twelfth International Conference on Cosmic Rays, Hobart, 1971 (unpublished).

⁸J. Nishimura, in *Encyclopedia of Physics*, edited by

S. Flügge (Springer, Berlin, 1967), Vol. XLVI/2, p. 1 ff.

⁹K. Ott, in *Kosmische Strahlung*, edited by Werner Heisenberg (Springer, Berlin, 1953).

¹⁰B. Rossi and K. Greisen, Rev. Mod. Phys. **13**, 249 (1941); B. Rossi, *High-Energy Particles* (Prentice-Hall, Englewood Cliffs, N. J., 1961).

¹¹H. H. Nagel, Z. Physik **186**, 319 (1965).

¹²U. Völkel, DESY Report No. 65/6, 1965 (unpublished).

¹³H. Burfeindt, DESY Report No. 67/24, 1967 (unpublished).

¹⁴H. Lengeler, W. Tejessy, and M. Deutschmann, Z. Physik **175**, 283 (1963).

¹⁵K. Pinkau, Phys. Rev. **139**, B1548 (1965).

¹⁶C. J. Crannell, H. Crannell, C. R. Gillespie, K. Pinkau, and R. R. Whitney, Phys. Rev. **182**, 1435 (1969).

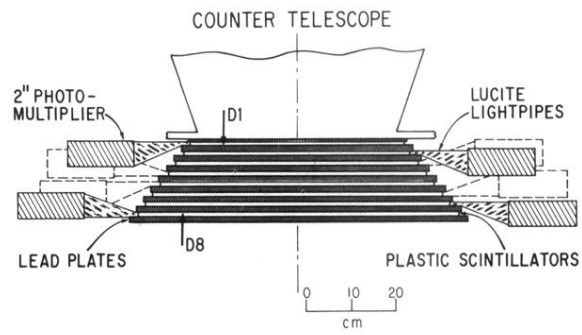


FIG. 1. Schematic cross section of the lead-scintillator sandwich. The detector is rotationally symmetric with respect to the central axis.